A WIRELESS, SMARTPHONE-AIDED MAGNETIC STRAIN SENSOR FOR BIOMEDICAL APPLICATIONS

Tianshuo Zhang[1,2], Manuel Ochoa [1,2], Rahim Rahimi[1,2], and Babak Ziaie[1,2]
[1]School of Electrical and Computer Engineering, Purdue University, West Lafayette, IN, USA
[2]Birck Nanotechnology Center, Purdue University, West Lafayette, IN, USA

ABSTRACT

This paper reports an implantable wireless strain sensor comprising laser-machined polymeric magnetic stripes embedded in a dual-silicone stretchable matrix. Each magnetic stripe is encapsulated in a stiffer PDMS package which is then embedded in a softer Ecoflex® band. This unique dual-silicone structure takes advantage of the elastic modulus mismatch between PDMS and Ecoflex®, significantly reducing the dislocation of magnetic stripes which may occur due to poor bonding while keeping the band stretchable. Strains within a physiological relevant range (e.g., cardiac cycle of 60–100 bpm, 40%–60% strain) can be picked up wirelessly by the magnetic sensor of a smartphone at 2.5 cm away, a distance practical for cardiovascular and pulmonary applications.

INTRODUCTION

Wireless measurement of physiological strain in specific tissues can provide significant diagnostic information regarding many important cardiovascular and pulmonary diseases. In particular, heart failure (HF), the inability of the heart to pump sufficient blood (a major public health issue [1]), can be evaluated by measuring cardiac tissue strain during the pumping cycle. Implantable haemodynamic monitoring systems, such as CardioMEMS™ HF system, can provide real-time cardiac pressure information that allows improved HF management, leading to fewer hospitalizations and lower medical expenditure [2]. However, such systems require complicated fabrication and custom-made, cumbersome interrogation systems [3]. A more modern alternative is the use of smartphones as a platform for collecting, transmitting and analyzing physiological parameters due to their portability (mobile computation power) and the integration of various physical sensors on board. Among the various sensing modes available via smartphones, magnetic tracking is a favorable option for implantable pressure, strain, or deformation sensing systems due to its size, passiveness, high sampling rate and the fact that human body imposes zero magnetic interference [4], [5].

In this paper, we present an implantable, passive magnetic strain sensing system with polymeric magnets that are laser-micromachined, re-magnetized and embedded into a carefully designed polydimethylsiloxane (PDMS) / Ecoflex® silicone composite band. The stiffer PDMS (elastic modulus 360–870 kPa) encapsulates the polymeric magnets while the softer Ecoflex® (elastic modulus 8.4 kPa) maintains the overall stretchability of the band. With such a configuration, this sensor is ideal as a monitor of heart strain. Figure 1 shows an illustration of the wireless heart monitoring system. The elastomeric strain sensor is sutured/glued onto the surface of the heart and strains/relaxes with each heartbeat. The separation of embedded polymeric magnetic stripes induces a change in magnetic field which can be detected via an external magnetic sensor and interpreted as a signal of cardiac strain. Magneto-static finite element analysis was performed to justify the sensor design. The strain sensing system was then calibrated within physiological relevant strain ranges. In strain cycles with frequency similar to that of the cardiac cycle, the resulting change in magnetic field due to the applied strain can be picked up wirelessly by a smartphone from a distance comparable to human chest wall thickness.

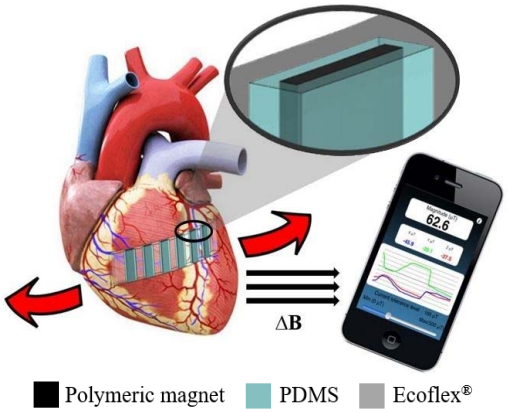

Figure 1: Schematic view of the wireless strain sensing system monitoring the strain of heart using a smartphone. Inset: enlarged view of the unique polymeric magnet/PDMS/Ecoflex® structure.

FABRICATION PROCESS

The fabrication of the magnetic strain sensor is illustrated in Figure 2. First, a commercial polymeric magnetic sheet ($SrFe_{12}O_{19}$ mixed with polyvinyl chloride (PVC) binder, 0.5 mm, Master Magnet) is temporarily bonded onto a silicon wafer (for handling during fabrication) and is subsequently laser-cut into 10 mm × 2 mm stripes using a 10.6 µm CO_2 laser (Universal Laser Systems, Scottsdale, AZ, USA), Figure 2a (wafer not shown). Excessive magnetic regions are removed and the stripes are cleaned with IPA, Figure 2b. Next, a 1 mm PDMS layer (Sylgard184, Dow Corning, 10:1) is casted on the sheet, Figure 2c. The polymeric magnet / PDMS double layer is then flipped, and another 0.5 mm PDMS layer is casted on top, completely encapsulating the polymeric magnetic stripes, Figure 2d. Once fully crosslinked, the PDMS layer is laser patterned into 0.5 mm thick encapsulations around each magnetic stripe, Figure 2e. Then, a 1 mm Ecoflex® layer

(0010, Smooth-On Inc., 1:1) is casted on both sides, filling the gap between polymeric magnet / PDMS isles and forming the stretchable regions, Figure 2f, g. Lastly the elastomeric band is released from the wafer and is magnetized in a vertical magnetic field from a neodymium permanent magnet (K&J Magnets, flux density B ≈ 1 T) for 1 minute, Figure 2h.

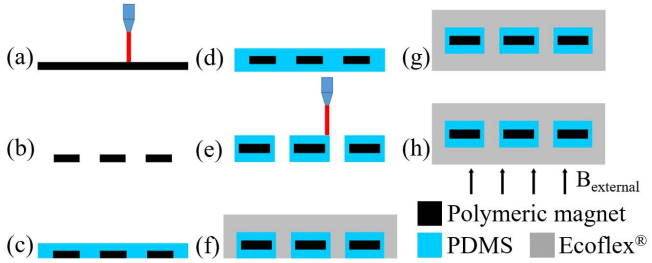

Figure 2: Fabrication process of the magnetic strain sensor. (a-b) Laser cut magnetic sheet into islands; (c-d) encapsulate stripes in PDMS; (e-g) laser machine into PDMS-magnet islands and encapsulate with Ecoflex®; (h) re-magnetize the band.

EXPERIMENTAL PROCEDURE

The magnetic strain sensor was characterized in terms of its remanence, coercivity, and relative permeability. The magnetic hysteresis loop of the magnetized polymeric magnetic stripes was measured by a superconducting quantum interference device (MPMS®3 SQUID, Quantum Design Inc., San Diego, CA, USA). Remanence (B_r) and relative permeability (μ_r) extracted from the hysteresis loop were then used for magneto-static finite element analysis (COMSOL, Burlington, MA, USA).

Strain sensors made of pure PDMS, pure Ecoflex® and PDMS/Ecoflex® composite were stretched on manipulator platform and maximum strain at delamination/break was measured.

PDMS/Ecoflex® composite strain sensors with separation of 4 mm, 6 mm and 8 mm between polymeric magnetic stripes were placed horizontally and stretched to various strains. The magnetic field-strain data was recorded by an AK8963 3-axis Hall effect sensor (Asahi Kasei, Tokyo, Japan) on board of an iPhone 6 (Apple Inc., Cupertino, CA, USA) from 2.5 cm away, a distance close to average chest wall thickness [6], via a magnetometer sensor log application (REGREX Co., Ltd.). The sensitivity of the Hall Effect sensor is 0.6 μT/LSB in 14-bit mode and 0.15 μT/LSB in 16-bit mode. The position of the magnetic sensor in the interior of the iPhone 6 is 2.0 cm from the top and 1.5 cm from the right edge, Figure 7a [7]. The physical region of the magnetic sensor was right above the center of the strain sensor during measurements.

RESULTS AND DISCUSSION

Magnetic Characterization

When acquired, the polymeric magnetic sheet was inherently magnetized in the Halbach array configuration. Halbach array, designed for augmenting the magnetic field on one side while canceling the field to near zero on the other, is a spatially rotating pattern of magnetization, Figure 3a. Seemingly ideal for the purpose of maximizing induced magnetic field, however, the Halbach array strengthens the near-field magnetic field by redirecting most of the magnetic field lines that should have extended deeply into space, weakening the far-field magnetic field. Applying a strong vertical magnetic field will re-align the magnetic domains and strengthen the far-field magnetic field, Figure 3b.

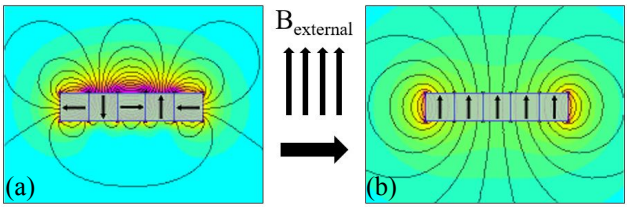

Figure 4: Magnetization and induced magnetic field in (a) Halbach array configuration, (b) uniform vertical configuration after exposed to a strong external magnetic field. Blue box indicates the unit cell of magnetization and the arrow indicates the direction of magnetization. (Source: K&J Magnets)

Magnetic property characterization is crucial to understanding the polymeric magnet's behavior after magnetization. Figure 4 shows the obtained magnetic hysteresis loop with vertical external field sweeping from H = -80×10^4 A/m (B ≈ -1 T) to 80×10^4 A/m (1 T). Remanence (B_r) is equal to the y-intercept value and the magnetic coercivity (H_c) is equal to the x-intercept value. Relative permeability (μ_r) is equal to the slope of the linear approximation equation near the magnetic intensity comparable to that inside human body (H = -10^4A/m to 10^4A/m) divided by the permeability of air (μ_0), Table 1.

Figure 5 shows the finite element analysis of magnetic flux density induced by a 4 mm-separation strain sensor at various strains. The color map indicates the base 10 logarithm of the magnitude of magnetic flux density ($\log_{10}|\vec{B}|$) while the arrow indicates the direction of flux density vector ($\vec{B}$). The

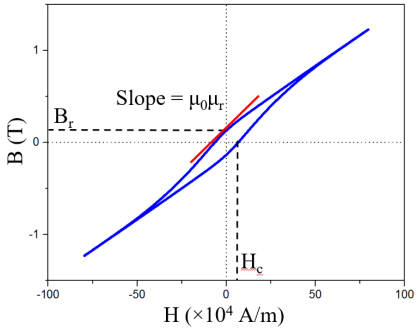

Figure 3: Magnetic hysteresis loop with vertical magnetic field sweep.

Table 1: Parameters obtained from hysteresis loop

Name	Symbol	Value	Unit
Remanence	B_r	0.131	T
Coercivity	H_c	1.5×10^5	A/m
Relative Permeability	μ_r	1.46	–

initial separation between each magnetic stripe is 4 mm and the strain sensor is then stretched to 40 % and 80 % strain. At 0 % strain the magnetic field of each stripe overlaps and adds up to a strong magnetic field, reaching 50 µT at 2.5 cm distance away, Figure 5a. At 40 % strain, the magnetic field of each stripe starts to separate and the resultant magnetic field at 2.5 cm drops to 25 µT, Figure 5b. At 80 % strain the magnetic field drops further to below 10 µT at 2.5 cm distance, Figure 5c.

Mechanical Characterization

Three strain sensor bands with identical dimensions but different separation between magnetic stripes (4 mm, 6 mm and 8 mm) were characterized, Figure 6a. Another two 6 mm strain sensors made from pure PDMS and pure Ecoflex® were used to justify the dual silicone band design, Figure 6b. Under the identical strain of 80 %, sensor made from pure Ecoflex® (elastic modulus 8.4 kPa) undergo magnet/Ecoflex® delamination while sensor made from pure PDMS (elastic modulus 870 kPa) ruptured. The stiffer PDMS acts as a trap for magnetic stripe, fixing it in place despite poor bonding along the interface. The softer Ecoflex® acts as the stretchable interconnections between each PDMS isle, keeping the entire band nearly as stretchable as pure Ecoflex® band. N. Naserifar et. al (2016) conducted finite element analysis and experimental characterization on a similar design that utilizes material gradients [8].

Sensor Calibration

Sensors with 4 mm separation between magnetic stripes exhibit the best sensitivity (1.13 µT / 10 %strain) thanks to denser magnetic stripe distribution but the least strain range (80 %) due to shorter stretchable Ecoflex® regions, Figure 7b. For sensors with greater initial separation between magnetic stripes (6 mm, 8 mm), their maximum strain increases (100%, 120%), accompanied by a decrease in induced magnetic field and strain sensitivity (0.98 µT / 10 %strain, 0.75 µT/ 10 %strain). The background magnetic flux density is around 55 µT. The strain sensor was able to monitor strain and heart rate within ranges relevant to cardiac cycle (40–60 % strain, 60–100 bpm), Figure 8a, b [9].

Biocompatibility

Materials used for this implantable strain sensor include PDMS, Ecoflex® and polymeric magnet (strontium ferrite with PVC binder). Both PDMS and Ecoflex® are nontoxic and biocompatible [10]. Strontium ferrite appears to be between "harmful" and "nontoxic" for aquatic organisms [11]. However, its cytotoxicity and biocompatibility for human are not well established. Industrial grade PVC binder inside polymeric magnet is not biocompatible but can be replaced with biocompatible medical grade PVC or polyethylene (PE) [12].

Conclusion

We developed an implantable, passive magnetic strain sensing system with polymeric magnets laser-

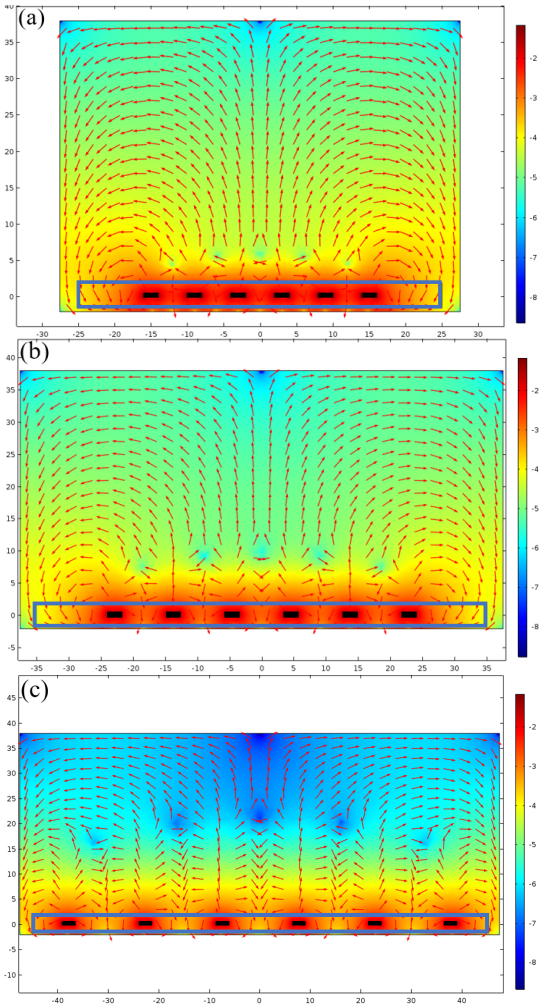

Figure 5: Magneto-static finite element analysis of a strain sensor at (a) 0% strain, (b) 40% strain and (c) 80% strain. The blue boxes are the sensor bands and the black boxes are the magnetic stripes. The color map indicates base 10 logarithmic of the magnitude of magnetic flux density ($log_{10}|\vec{B}|$) while the arrow indicates the direction of flux density vector ($\vec{B}$). Scale bar for the color map has a unit of T and the xy coordinates have a unit of mm.

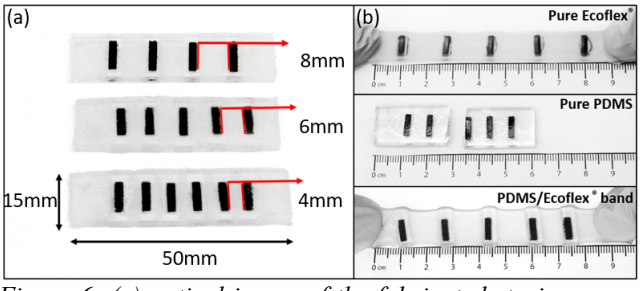

Figure 6: (a) optical image of the fabricated strain sensors with 4mm, 6mm and 8mm separation between polymeric magnets, (b) under 90% strain, pure Ecoflex® sensor underwent magnet/Ecoflex® delamination (top); pure PDMS sensor ruptured (middle); the dual silicone sensor functioned normally (bottom), separation between the magnetic stripes is 6mm in all three bands of different material.

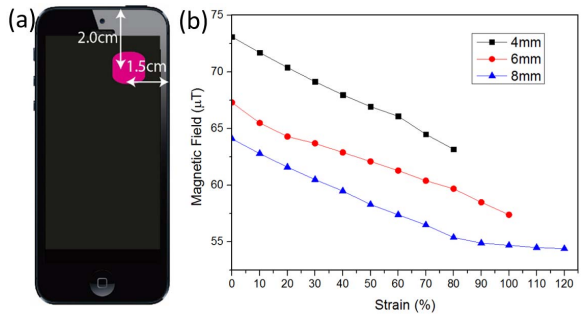

Figure 7: (a) Location of the magnetic sensor of an iPhone 6, (b) Magnetic field vs. strain calibration for the three sensor designs.

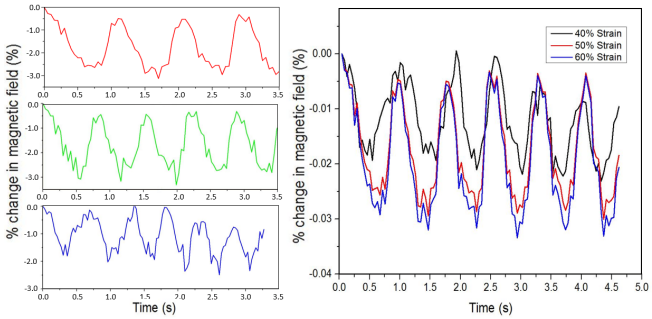

Figure 8: Response of a 4 mm sensor to cardiac cycle conditions: (a) transient response of % change in magnetic field under normal strain of heart (50 %) but at a strain rate equivalent to 60 bpm (red), 80bpm (green) and 100bpm (blue), (b) transient response of % change in magnetic field under various strains at a rate of 75 bpm.

micromachined, re-magnetized and embedded into a carefully designed PDMS/Ecoflex® silicone composite band. The stiffer PDMS encapsulates the polymeric magnets while the softer Ecoflex® fills the gap between PDMS regions. This unique composite structure utilizes stiffness gradient, preventing magnet delamination from elastomer matrix while maintaining overall stretchability. Magneto-static finite element analysis and strain experiments were performed to justify the magnetic and mechanical aspect of the sensor design. The strain sensing system was then calibrated within physiological relevant strain ranges. Cardiac cycle relevant strains (60–100 bpm, 40–60 % strain) can be measured wirelessly by a smartphone from 2.5 cm away, a distance comparable to average human chest wall thickness, with a sensitivity of 1.13 μT/10 % strain.

ACKNOWLEDGEMENTS

The authors thank Mr. Punyashloka Denashis, Dr. Neil R. Dilley and Prof. Zhihong Chen for their help on magnetic property measurements. The authors also thank the staff of the Birck Nanotechnology Center for their support. Funding for this work was provided in part by NextFlex PC 1.0.

REFERENCES

[1] A. L. Bui, T. B. Horwich, G. C. Fonarow, "Epidemiology and Risk Profile of Heart Failure", *Nat. Rev. Cardiology*, vol. 8(1), pp. 30-41, 2011.

[2] W. T. Abraham, P. B. Adamson, R. C. Bourge, M. F. Aaron, M. R. Costanzo, L. W. Stevenson, W. Strickland, S. Neelagaru, N. Raval, S. Krueger, S. Weiner, D. Shavelle, B. Jeffries, J.S. Yadav, "Wireless Pulmonary Artery Haemodynamic Monitoring in Chronic Heart Failure: A Randomized Controlled Trial", *Lancet*, vol. 377, pp. 658-666, 2011.

[3] F. Cros, D. O'Brien, M. Fonseca, M. Abercrombie, J. W. Park, A. Singh, US Patent 7621036 B2, 2009.

[4] E. L. Tan, B. D. Pereles, B. Horton, R. Shao, M. Zourob, K. G. Ong, "Implantable Biosensors for Real-time Strain and Pressure Monitoring", *Sensors*, vol. 8, pp. 6396-6406, 2008.

[5] S. Song, N. S. Race, A. Kim, T. Zhang, R. Shi, B. Ziaie, "A Wireless Intracranial Brain Deformation Sensing System for Blast-Induced Traumatic Injury", *Scientific Reports*, vol. 5, 16959, 2015.

[6] A. R. McLean, M. E. Richards, C. S. Crandall, J. L. Marinaro, "Ultrasound Determination of Chest Wall Thickness: Implicaitons for Needle Thoracostomy", *The American J. of Emergency Medicine*, vol. 29, pp. 1173-1177, 2011.

[7] E. Arribas, I. Escobar, C. P. Suarez, A. Najera, A. Belendez, "Measurement of Magnetic Field of Small Magnets with A Smartphone: A Very Economical Laboratory Practice for Introductory Physics Courses", *European J. of Physics*, vol. 36(6), 2015.

[8] N. Naserifar, P. R. LeDuc, G. K. Fedder, "Material Gradients in Stretchable Substrates Toward Integrated Electronic Functionality", *Adv. Mater.*, vol. 28, pp. 3584-3591, 2016.

[9] A. M. Maceira, S. K. Prasad, M. Khan, D. J. Pennell, "Reference Right Ventricular Systolic and Diastolic Function Normalized to Age, Gender and Body Surface Area from Steady-State Free Precession Cardiovascular Magnetic Resonance", *European Heart J.*, vol. 27, pp. 2879-2888, 2006.

[10] G. Park, H. Chung, K. Kim, S. A. Lim, J. Kim, Y. Kim, Y. Liu, W. Yeo, R. Kim, S. S. Kim, J. Kim, Y. H. Jung, T. Kim, C. Yee, J. A. Rogers, K. Lee, "Immunologic and Tissue Biocompatibility of Flexible/Stretchable Electronics and Optoelectronics", *Adv. Healthcare Mater.*, vol. 3, pp. 515-525, 2014.

[11] C. Blaise, F. Gagne, J. F. Ferard, P. Eullaffroy, "Ecotoxicity of Selected Nano-Materials to Aquatic Organism", *Environmental Toxicology*, vol. 23, 591-598, 2008.

[12] E. A. E. Van Tienhoven, D. Korbee, L. Schipper, H. W. Verharen, W. H. De Jong, "In Vitro and in Vivo (Cyto)toxicity assays using PVC and LDPE as model materials", *J. of Biomed. Mater. Research*, vol. 78A(1), pp. 175-182, 2006.

CONTACT

*T. Zhang, tel: +1-765-4181366;
zhan1476@purdue.edu